JCTC Journal of Chemical Theory and Computation

ARTICLE

pubs.acs.org/JCTC

Addressing Methionine in Molecular Design through Directed Sulfur−Halogen Bonds

Rainer Wilcken,[†] Markus O. Zimmermann,[†] Andreas Lange,[†] Stefan Zahn,[‡] Barbara Kirchner,[‡] and Frank M. Boeckler[†,*]

[†]Laboratory for Molecular Design and Pharmaceutical Biophysics, Department of Pharmaceutical and Medicinal Chemistry, Institute of Pharmacy, Eberhard-Karls-University Tübingen, Auf der Morgenstelle 8, 72076 Tübingen, Germany

[‡]Wilhelm-Ostwald-Institut für Physikalische und Theoretische Chemie, Universität Leipzig, Linnéstr. 2, 04103 Leipzig, Germany

Supporting Information

ABSTRACT: Halogen bonds are directional interactions involving an electron donor as binding partner. Employing quantum chemical calculations, we explore how they can be used in molecular design to address the sulfur atom in a methionine residue in a previously neglected, directed manner. We characterize energetics and directionality of these halogen bonds and elucidate their spatial variability in suboptimal geometries that are expected to occur in protein−ligand complexes featuring a multitude of concomitant interactions. We derive simple rules allowing medicinal chemists and chemical biologists to easily determine preferred areas of interaction within a binding site and to exploit them for scaffold decoration and design. Our work shows that sulfur−halogen bonds may be used to expand the patentable medicinal chemistry space. We demonstrate their potential to increase binding affinities and suggest that they can significantly contribute to inducing and tuning subtype selectivities.

INTRODUCTION

A profound understanding of molecular recognition is the essential basis of structure-based molecular design. Established protein−ligand interactions such as hydrogen bonds and hydrophobic contacts have been increasingly complemented by nonclassical interaction types such as $\pi-\pi$ or cation$-\pi$ contacts which may play important roles and contribute substantially to total binding affinity. However, very few of these nonclassical interaction types have so far been included in common molecular design tools, as emphasized in a recent review.[1]

Among these often neglected interactions is halogen bonding, an attractive interaction of the type R−X···D−R′, where X represents chlorine, bromine, or iodine and D can be any kind of Lewis base. This interaction has been broadly recognized in materials sciences since the 1970s,[2,3] but its occurrence in biological systems has been studied only recently, e.g., through statistical PDB evaluations.[4] The driving force of the interaction can be explained within the σ-hole concept: the halogen atoms possess a characteristic crown of positive charge due to a deficiency in electron density in the outer lobe of the p_z orbital (where z is chosen as the R−X axis).[5−9] The σ-hole concept has been extended and applied to group VI atoms, which can be relevant in biological systems.[10,11] Several quantum chemical studies using small model systems have been performed to characterize the nature and strength of halogen bonds.[12,13] QM/MM calculations on protein−ligand complexes have also been conducted[14,15] and similarities as well as differences between halogen bonding and hydrogen bonding have been discussed.[16−19] Halogen bonds involving backbone carbonyl oxygen atoms have been implicated as favorable interactions by some very recent experimental studies.[20,21]

When searching the PDB for ligand−protein halogen-bond contacts, as done in a recent study,[15] mainly two types of halogen bonds are observed—contacts to backbone carbonyl moieties (53%) and halogen$-\pi$ contacts (33%)—while those involving sulfur or nitrogen are found only sparsely (5% S, 9% N). However, this does not mean that sulfur−halogen bonds are unfavorable. Most ligand−protein halogen bonds observed in the PDB were not rationally designed but found serendipitously due to the nonclassical nature of this contact. Thus, it is likely that halogen−sulfur contacts are merely underrepresented given the number of carbonyl oxygen moieties in a protein. We demonstrate that addressing the sulfur-containing side chain of methionine through halogen bonds has distinct potential for improving affinity and selectivity of a compound.

In this work, we use quantum chemical calculations at the DFT-D, MP2, and CCSD(T) level and large basis sets to characterize the interaction strengths between ligand model systems and three different molecular representations of methionine. Where possible, we make sure to obtain interaction geometries and energies that solely represent the halogen-bond contact, avoiding additional secondary interactions. From our model calculations, we deduce simple rules on how to best address methionine through halogen bonding. Additionally, we focus on elucidating the impact of deviations from ideal binding geometries on overall complex formation energies. Finally, we show that our model calculations agree well with an existing crystal structure of IL-2[22] and propose a way to visualize favorable areas of interaction within a binding site, making our results immediately applicable for use in molecular design.

RESULTS

Energetics of the Halogen Bond. We represent methionine as a molecular system of three different sizes: (i) as the simple model

Received: April 8, 2011
Published: June 02, 2011

system dimethyl sulfide (MET1); (ii) as 1-(methylsulfanyl)propane (MET2), representing the complete methionine side chain including Cα; and (iii) as full amino acid including backbone atoms, capped by an acetyl group at the N-terminus and a *N*-methyl amide at the C-terminus (MET3) (Figure 1). Input geometries for MET2 and MET3 were extracted from 3DN4, a PDB structure featuring a short iodine−methionine contact.[23] The backbone conformation of MET3 is α-helical with $\varphi = -59.9°$ and $\psi = -47.5°$, and the side chain conformation is gauche(−)−trans−gauche(+). We have restricted the φ and ψ angles in all optimizations involving MET3 to avoid biologically unreasonable backbone conformations. We employ iodobenzene, bromobenzene, and chlorobenzene as ligand models because substituted aromatic or heteroaromatic scaffolds are common cores in medicinal chemistry and their halogenation may be exploited for scaffold decoration.

Using the small methionine model MET1, we obtain optimized halogen-bonded complexes for all three halobenzenes at the MP2/QZVPP level. Interaction energies are calculated as adduct formation of the halogen-bonded complex from isolated halobenzene and methionine (Table 1). We observe the strongest interaction (−19.3 kJ/mol) for the iodobenzene complex, while bromobenzene and chlorobenzene complexes show weaker interaction energies (−13.0 and −10.1 kJ/mol, respectively). This order of halogen-bond strengths (Cl < Br < I) has been reported numerous times in the literature, regardless of the Lewis base

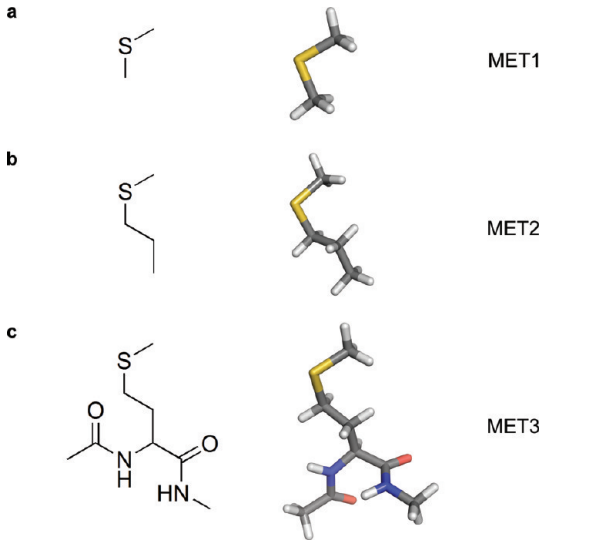

Figure 1. Methionine model systems MET1 (a), MET2 (b), and MET3 (c), represented as structural formulas and stick models (optimized geometries).

interaction partner.[9,19] In our calculations, all halogen bonds show X···S distances below the sum of van der Waals radii of the two atoms. Despite the size of iodine, the I···S bond is the shortest, implying a very favorable interaction. Interestingly, the equilibrium distances for all X···S bonds are quite similar (around 3.4 Å), indicating that a substitution of chlorine by one of the other two halogens should be feasible despite the differences in size. Employing widely used density functionals augmented by an empirical dispersion correction (DFT-D), we find that some of these quite closely mimic the results obtained with MP2 (Supporting Information, Table S1). To describe the strength of an iodine−sulfur halogen bond with chemical accuracy, we perform CCSD(T) calculations by employing a basis set extrapolation scheme (see Methods, eqs 1 and 2 and Supporting Information Table S2) and obtain an interaction energy of −17.3 kJ/mol. This is reasonably close to our MP2 results.

To put the halogen-bond energies into context, we model two H···S interactions formed by benzene and MET1 (weak hydrogen bond) as well as phenol and MET1 (moderately strong hydrogen bond) at MP2/QZVPP level. Benzene forms a complex with MET1 at a much reduced bond distance compared to the halobenzenes (279 vs 336 pm, H vs I), with a complex formation energy of −11.0 kJ/mol. The phenol−MET1 complex shows the largest interaction energy of all investigated model systems (−29.1 kJ/mol).

However, adding just one water molecule to the adduct formation reaction for the sake of introducing ligand desolvation energies changes the overall picture dramatically. If we require the ligand to be desolvated upon binding, i.e., if we exchange ligand-bound water by ligand-bound methionine (Figure 2), the reaction energy for phenol is reduced to −1.4 kJ/mol. In contrast, the iodobenzene and benzene reaction energies are only reduced to −11.3 and −6.0 kJ/mol, respectively. This one-molecule approach to solvation is rather simplistic but helps illustrate how desolvation energies can differ between nonpolar and polar ligands. To complete the energetic description of the methionine−halogen bond, we perform geometry optimizations on the larger methionine model systems MET2 and MET3. Switching from the quadruple-ζ basis set (QZVPP) to the smaller triple-ζ basis TZVPP due to computational considerations for the larger models, we obtain smaller interaction energies for all halogen-bonded systems, implying that the MP2 method heavily depends on basis set size. Expanding the methionine in size from MET1 to MET2 and MET3, we observe a moderate rise in interaction energies while retaining virtually unchanged geometries (Supporting Information, Figure S1, Table 2). For the treatment of the chlorobenzene···MET3 adduct, we had to additionally restrict the bond angle $\alpha_{S5-Cl6-C7}$ during optimization to obtain a halogen-bonded geometry.

Table 1. Interaction Energies (in kJ/mol) for Halogen-Bonded Model Complexes (small methionine model system MET1)[a]

complex	ΔE	method	$d_{S5-X6/H6}$, pm (% vdW[b])	$\alpha_{C4-S5-X6/H6}$, deg	$\delta_{C3-C4-S5-X6/H6}$, deg	$\alpha_{S5-X6/H6-C7/O7}$, deg
$C_6H_5I\cdots$MET1	−19.3	MP2/QZVPP	336 (88.9)	88.8	−88.6	169.8
$C_6H_5Br\cdots$MET1	−13.0	MP2/QZVPP	343 (94.0)	85.9	−85.2	170.1
$C_6H_5Cl\cdots$MET1	−10.1	MP2/QZVPP	348 (98.0)	80.9	−79.6	162.7
$C_6H_6\cdots$MET1	−11.0	MP2/QZVPP	279 (96.2)	79.3	77.3	156.9
$C_6H_5OH\cdots$MET1	−29.1	MP2/QZVPP	226 (77.9)	86.8	−86.1	153.8
$C_6H_5I\cdots$MET1	−17.3	CCSD(T)/CBS[c]	345 (91.3)	88.8	−88.5	168.4

[a] Interaction energies for complex formation with benzene and phenol (H···S contacts) are given for comparison. Energies were corrected for BSSE using the counterpoise correction. [b] Percentage of the sum of the van der Waals radii of the two atoms directly involved in bonding. [c] CCSD(T) calculations were performed on the SCS-MP2/QZVPP minimum geometry and a basis set extrapolation scheme was employed (see Methods).

In summary, we find that methionine can be favorably addressed through halogen bonds, especially by those involving Br···S or I···S contacts. Taking into account desolvation penalties implies that these interactions might be superior to weak and moderately strong hydrogen bonds. Interestingly, while most halogen bonds in the PDB are formed by ligands with chloro substituents, our data reconfirm earlier studies, demonstrating that exchange of these chlorines by bromine or iodine is feasible and energetically favorable.

Distance Dependencies of Halogen Bonds. In existing crystal structures, the optimal geometries described above are not always observed due to the interplay of multiple competing primary and secondary interactions involved in ligand binding. For this reason, we investigate the influence of nonideal bond distances on complex formation energy. Starting from MP2/TZVPP minimum structures, we perform distance scans along the X···S bond. The scans are carried out as single point calculations using methionine model MET1 as all three methionine systems show very similar behavior in terms of energetics and distance dependence (Supporting Information, Figure S2).

In rational drug design, introducing an additional moiety like a halogen atom into a lead structure makes most sense if it leads to an affinity increase. We have demonstrated that halogen bonds are favorable interactions. However, we have to keep the "background affinity" in mind that is already provided by an H···S contact in an ideal halogen-bond distance, representing an undecorated benzene scaffold. We thus have to compare the complex formation energy of the halobenzene−methionine complexes with the benzene−methionine complex at the ideal halogen bond distance. This distance is very similar for all three halogenated complexes (339, 343, and 347 pm for I, Br, and Cl at the MP2/TZVPP level). Figure 3 shows the distance dependence of the complex formation energies. At 339 pm, the complex formation energy for benzene is ΔE(MP2/TZVPP) = −8.7 kJ/mol. We use this energy as a threshold: The introduction of a halogen into the ligand structure at any distance $d_{X\cdots S}$ needs to be energetically more favorable than 8.7 kJ/mol in order to improve binding energy. This definition (horizontal line in Figure 3b) leads to areas of tolerance for all three halobenzene

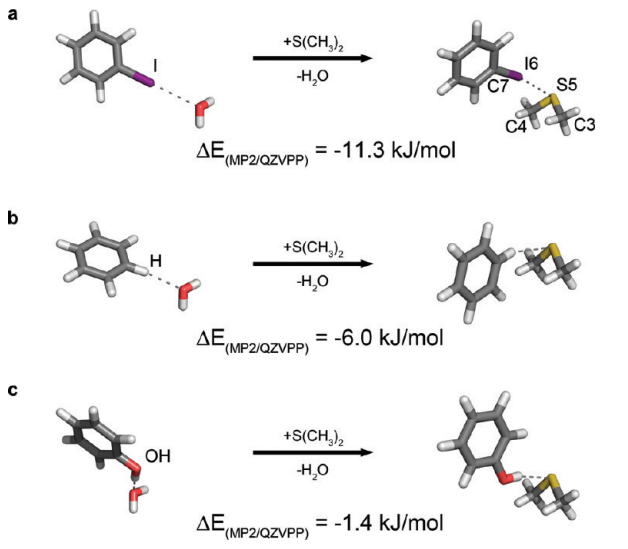

Figure 2. Reactions representing ligand desolvation: Exchange of water from iodobenzene···water (a), benzene···water (b), and phenol··· water (c) complexes by dimethyl sulfide (MET1) and corresponding reaction energies (kJ/mol) at the MP2/QZVPP level. These three model systems represent (a) halogen bonds and (b) weak and (c) moderately strong hydrogen bonds. Relevant atom labels, which are used for defining distances, angles, and dihedrals, are shown in the iodobenzene···MET1 complex (a).

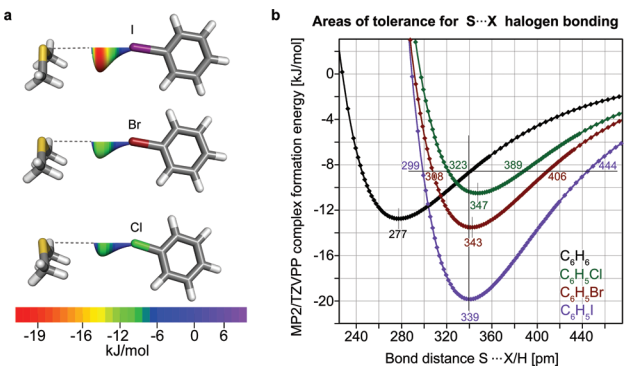

Figure 3. (a) Distance scan plots for the three halobenzene···MET1 complexes. The curves depicted in the model systems highlight preferred regions of halogen placement by their coloring and size. (b) Plot of X···S (H···S) distance vs complex formation energy for iodobenzene, bromobenzene, chlorobenzene, and benzene complexes with MET1 (MP2/TZVPP) and definition of areas of tolerance for the halobenzene···methionine complexes.

Table 2. Interaction Energies (in kJ/mol) for Adduct Formation Yielding Halogen-Bonded Complexes with the Three Methionine Models at MP2/TZVPP Level[a]

complex	$\Delta E_{MP2/TZVPP}$	d_{S5-X6}, pm	$\alpha_{C4-S5-X6}$, deg	$\delta_{C3-C4-S5-X6}$, deg	$\alpha_{S5-X6-C7}$, deg
$C_6H_5I\cdots$MET1	−15.2 (−19.8)	339	88.3	−88.0	169.5
$C_6H_5I\cdots$MET2	−16.2 (−21.2)	339	88.3	−87.0	170.3
$C_6H_5I\cdots$MET3	−16.6 (−21.7)[b]	342	88.9	−84.2	168.1
$C_6H_5Br\cdots$MET1	−10.7 (−13.5)	343	85.8	−85.1	170.1
$C_6H_5Br\cdots$MET2	−11.2 (−14.1)	342	85.6	−85.2	172.0
$C_6H_5Br\cdots$MET3	−12.6 (−15.6)[b]	347	84.7	−80.2	163.7
$C_6H_5Cl\cdots$MET1	−7.8 (−10.5)	347	80.9	−79.5	162.7
$C_6H_5Cl\cdots$MET2	−8.2 (−11.1)	348	80.1	−79.6	163.6
$C_6H_5Cl\cdots$MET3	−10.0 (−13.1)[b,c]	349	80.6	−75.9	162.4

[a] Energies are counterpoise-corrected; uncorrected energies are given in brackets. [b] Methionine model system MET3 was extracted from PDB structure 3DN4, and backbone φ and ψ dihedrals were frozen in the original α-helical geometry. [c] For the chlorobenzene···MET3 complex, the bond angle $\alpha_{S5-Cl6-C7}$ was constrained to 162.4° to obtain a halogen-bonded minimum structure.

Table 3. Comparison of the MP2/TZVPP Complex Formation Energies (in kJ/mol) at Optimal Distances and at the Equilibrium Distance of Iodobenzene···MET1 Yields Distance Areas of Tolerance[a]

		$\Delta E_{MP2/TZVPP}$		
complex	$d_{S5-X6/H6}$, pm	at optimal distances	at 339 pm	areas of tolerance for $d_{S5-X6/H6}$, pm
$C_6H_5I\cdots$MET1	339	−19.8	−19.8	299−444
$C_6H_5Br\cdots$MET1	343	−13.5	−13.5	308−406
$C_6H_5Cl\cdots$MET1	347	−10.5	−10.4	323−389
$C_6H_6\cdots$MET1	277	−12.7	−8.7	N/A

[a] All halogen-bonded complexes with S···X distances within tolerance have interaction energies greater than 8.7 kJ/mol, which is the complex formation energy of benzene···MET1 at 339 pm.

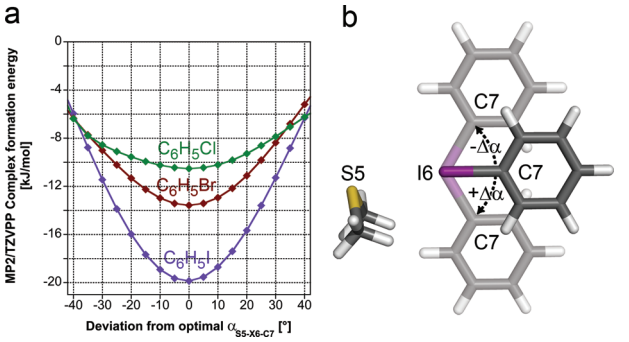

Figure 4. (a) Impact of deviations from optimal σ-hole angles $\alpha_{S5-X6-C7}$; energies are calculated using MP2/TZVPP. (b) Illustration of scan setup: the ligand model system is rotated around the axis perpendicular to the paper plane passing through I6.

ligand systems (presented in detail in Table 3). For chlorobenzene, the area of tolerance reaches from 323 to 389 pm, and the energy gain is at most 1.8 kJ/mol compared to benzene (at the ideal bond distance of 343 pm). While this explains the occurrence of some Cl···S halogen bonds in the PDB, it also illustrates that there is no big affinity increase to be expected by simply exchanging H for Cl at one position on a benzene-based scaffold, unless this interaction is supplemented by other interactions that the chlorine may participate in. For bromobenzene, the area of tolerance becomes larger (308−406 pm) and the energy gain more pronounced. For the iodobenzene complex, the distance tolerance is especially large (299−444 pm), with a favorable complex formation energy of less than ΔE(MP2/TZVPP) = −18 kJ/mol within a range of about 320−365 pm.

In addition to the MP2 method, we also carried out the distance scans employing four widely used density functionals (BP86-D, BLYP-D, B3LYP-D, and TPSS-D, Supporting Information, Figure S3). TPSS-D shows the best agreement with the MP2 data while being much less computationally expensive.

The agreement of our distance scans with experimental data is exemplified in two crystal structures from the PDB containing iodine−sulfur halogen bonds. For 3DN4,[23] the authors report a bond distance of 3.3 Å, while for 2PIW, the thyroid hormone 3,3′,5-triiodo-L-thyronine is bound to the androgen receptor[24] with an S···I distance of 3.7 Å. Both distances are well within our areas of tolerance.

Energetic Impact of σ-Hole Bond Directionality. It is generally agreed that the driving force of halogen bonding is the σ-hole, a crown of positive charge on chlorine, bromine, and iodine residues. The σ-hole concept explains halogen bonding as an electrostatic interaction similar to hydrogen bonding.[5,19] One study has suggested that halogen bonds may be driven by both electrostatic and dispersive forces, using symmetry-adapted perturbation theory.[12]

A purely electrostatics-driven interaction would translate into a very directional bond, meaning that deviations from the ideal bond angle $\alpha_{S5-X6-C7}$ would be heavily penalized. If the interaction was mainly driven by dispersion, one would expect more undirected, "greasy" behavior, and deviations from the ideal angle would be tolerated to a large extent. These two scenarios are decisively different and have great impact in molecular design approaches, e.g., in scaffold placement. In the dispersion-driven case, the scaffold and the halogen solely need to be placed in the right distance from a methionine residue, while in the electrostatics-driven case, both the distance $d_{X6\cdots S5}$ and the angle $\alpha_{S5-X6-C7}$ are very important and need to be matched as closely as possible.

To evaluate the energetic penalties of nonideal σ-hole bond angles, we first optimize the halobenzene···MET1 dimer constrained to C_s symmetry at the MP2/TZVPP level in order to rule out any secondary interactions of the aromatic ring with the methyl moieties of the MET1 system. The resulting complexes possess $\alpha_{S5-X6-C7}$ angles of 168.5° (I), 166.9° (Br), and 162.6° (Cl). We then successively change the bond angle $\alpha_{S5-X6-C7}$ in 5° steps and perform MP2/TZVPP single point calculations. The results of the scans are shown in Figure 4a, with a schematic representation of positive (+Δα) and negative (−Δα) deviations from ideal (C_s) geometry given in Figure 4b. Interestingly, even though the strengths of the halogen bonds for the three halobenzenes are very different, as discussed earlier, the derived tolerance areas are similar at about ±30° deviation from ideal angles. It is important to note that the potential curves are fairly symmetric, even though the "optimized" angle is not 180°. Another surprise is that the curves cross at about ±40°, which means that at this angle, there is no advantage of substituting one halogen for another. From these scans, we derive that halogen bonds are strongly directional and that large deviations from the ideal $\alpha_{S5-X6-C7}$ angle have the potential to ruin binding affinities, especially in the case of the favorable I···S interaction. This confirms the electrostatics-driven nature of the interaction and is in accordance with studies on other model systems.[18] Deviations from the ideal angle amounting to more than 20°−30° should be avoided at all costs, and scaffolds should be selected (e.g., in a scaffold-hopping approach) or designed de novo to allow for close to optimal (≈170°) $\alpha_{S5-X6-C7}$ angles.

Dihedral Angle Variations—Spherical Scans. Taking one step toward integrating halogen bonds in molecular design tools, we investigate degrees of freedom in the spherical orientation of the halogen with respect to the methionine sulfur. Starting from an optimized input geometry and using 5° steps in varying the angles (see Methods), we generate 2664 variations of the interaction geometry, keeping the halogen at the equilibrium distance on a sphere around the sulfur atom as its center. We prepare the input geometry by conducting a constrained optimization (MP2/TZVPP) in C_s symmetry with the bond angle $\alpha_{S5-X6-C7}$ restricted to 180° and the dihedral angle $\delta_{C3-C4-S5-X6}$ restricted to 90° to avoid unsymmetric artifacts due to bias in the input structure. This bias arises predominantly from the deviation of the σ-hole angle $\alpha_{S5-X6-C7}$ from 180° in the optimized structure. The constraints

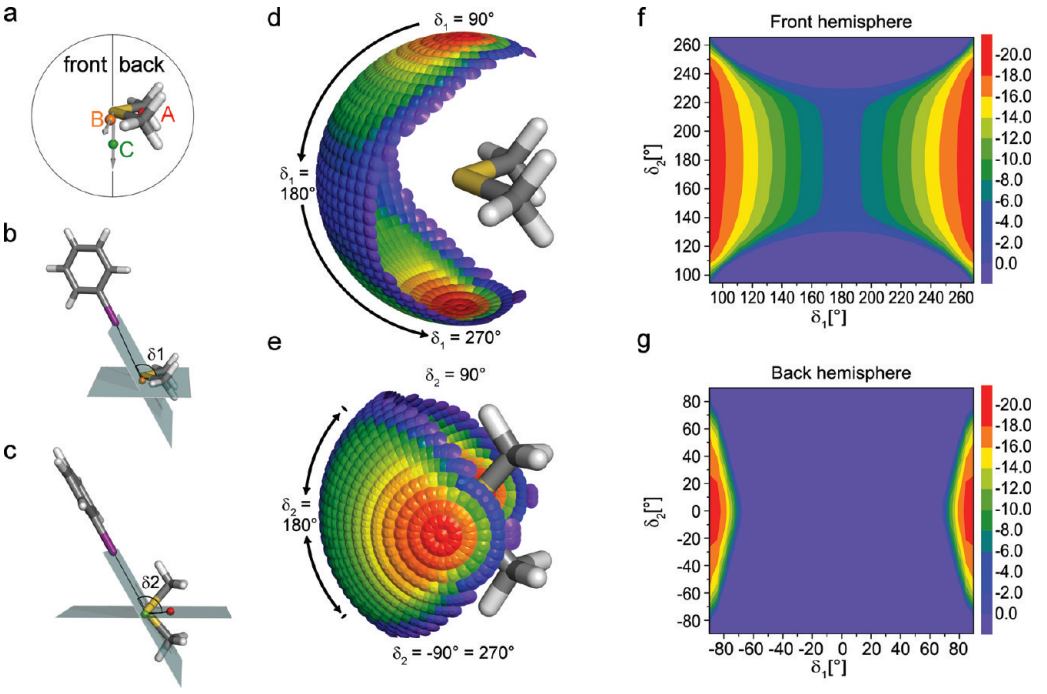

Figure 5. Spherical scans for iodobenzene. (a) Definition of front and back hemisphere for MET1 and position of dummy points A−C used to define dihedral angles. Positions of dummy points B and C are highlighted by vectors centered at S5. (b) Illustration of dihedral angle δ_1 (out-of-plane rotation). δ_1 represents the rotation around an axis through dummy point B and atom S5, which is part of the C−S−C plane and is oriented perpendicularly to the mirror plane of the methionine fragment. (c) Illustration of dihedral angle δ_2 (in-plane rotation). δ_2 represents the rotation around an axis from dummy point C to atom S5, which is oriented perpendicularly to the C−S−C plane. (d) Interaction energy sphere for the iodobenzene···MET1 complex, oriented to exemplify variations in δ_1. (e) Interaction energy sphere for iodobenzene···MET1 complex, oriented to exemplify variations in δ_2. (f, g) 2D plots (δ_1 vs δ_2) of interaction energies on the front hemisphere (f) and back hemisphere (g).

have a mild impact on energies compared to the freely optimized complexes (1.1 kJ/mol for iodobenzene···MET1, 1.2 kJ/mol for bromobenzene···MET1, 2.0 kJ/mol for chlorobenzene···MET1; overlays of constrained and freely optimized structures are shown in the Supporting Information (Figure S4). The cutoff for the areas of tolerance changes to −6.4 kJ/mol as the same constraints are applied to the benzene···MET1 complex. We conduct the spherical scans with the more efficient DFT-D method TPSS-D/TZVPP, which delivers interaction energies comparable to the more expensive MP2/TZVPP method as exemplified in the distance scans (Supporting Information, Figure S3).

The obtained interaction sphere for iodobenzene···MET1 is presented in Figure 5d,e from two different perspectives. These perspectives are chosen to focus on variations of the two dihedral angles δ_1 (=$\delta_{C4-B-S5-X6}$) and δ_2 (=$\delta_{A-C-S5-X6}$) as defined in Figure 5, parts b and c, respectively. While Figure 5b,d highlights the variation of the "out-of-plane" δ_1 angle, changes in the "in-plane" δ_2 angle are more easily perceived from Figure 5c,e. The plane is defined by the three heavy atoms (C−S−C) of the methionine fragment. To emphasize the areas of tolerance regarding the dihedrals δ_1 and δ_2, we present 2D plots for the interaction areas on the front and back hemisphere in Figure 5f,g. A definition of front and back hemisphere is given in Figure 5a.

In order to deduct simple rules, we discuss particular points on the sphere indicative of general trends. Starting from the input geometry of the sphere, we first focus on the variation of the δ_1 angle from 90° out-of-plane toward in-plane (δ_1 = 180°) and further toward 270°, while keeping δ_2 = 180° (i.e., placing the iodine right in front of the sulfur atom). In Figure 5d, this corresponds to starting from the red area above MET1 and proceeding down along the circular path to the red area below MET1 (black arrow). In Figure 5f, this circular path becomes a straight line from the left to the right at δ_2 = 180°. We observe a significant loss of interaction energy toward only −4 to −6 kJ/mol remaining for the in-plane geometry (δ_1 = 180°, δ_2 = 180°). Thus, there is a strong energy dependence on changes in δ_1, with out-of-plane angles close to ±90° being highly favored over in-plane geometries. It becomes much more pronounced when we look at the back of the sphere (Figure 5g). As this hemisphere includes both methyl groups of the methionine, the decrease in energy is much more rapid and results in numerous sterical clashes, leaving just a small tolerance area between δ_1 = 80° and 90° or −80° and −90°.

In contrast to the large impact of changes in δ_1, it is easily possible to vary δ_2 within as much as ±40° from the 180° geometry. This can be observed particularly well in Figure 5e, where the symmetry with respect to δ_2 = 180° becomes obvious. As we proceed down the sphere from the red area (corresponding to changes in δ_1), the coloring at different δ_2 angles (proceeding circularly along each "δ_1 level") is identical to a large extent.

For the lighter halogens chlorine and bromine, the interaction spheres show strongly attenuated energies of complex formation. Thus, Figure 6a,d (as well as corresponding 2D plots in Figure 6b,c, e,f) gives a quantitatively different, but qualitatively similar, impression when compared to the iodine figures. As the halogen bond strength to the sulfur atom of methionine is much weaker for the lighter halogens, the preferred interaction areas are much smaller than for iodine. While there is still a reasonably large interaction area for bromobenzene···MET1, the area for chlorobenzene shrinks to only those data points close to the optimal interaction geometry.

dx.doi.org/10.1021/ct200245e |J. Chem. Theory Comput. 2011, 7, 2307–2315

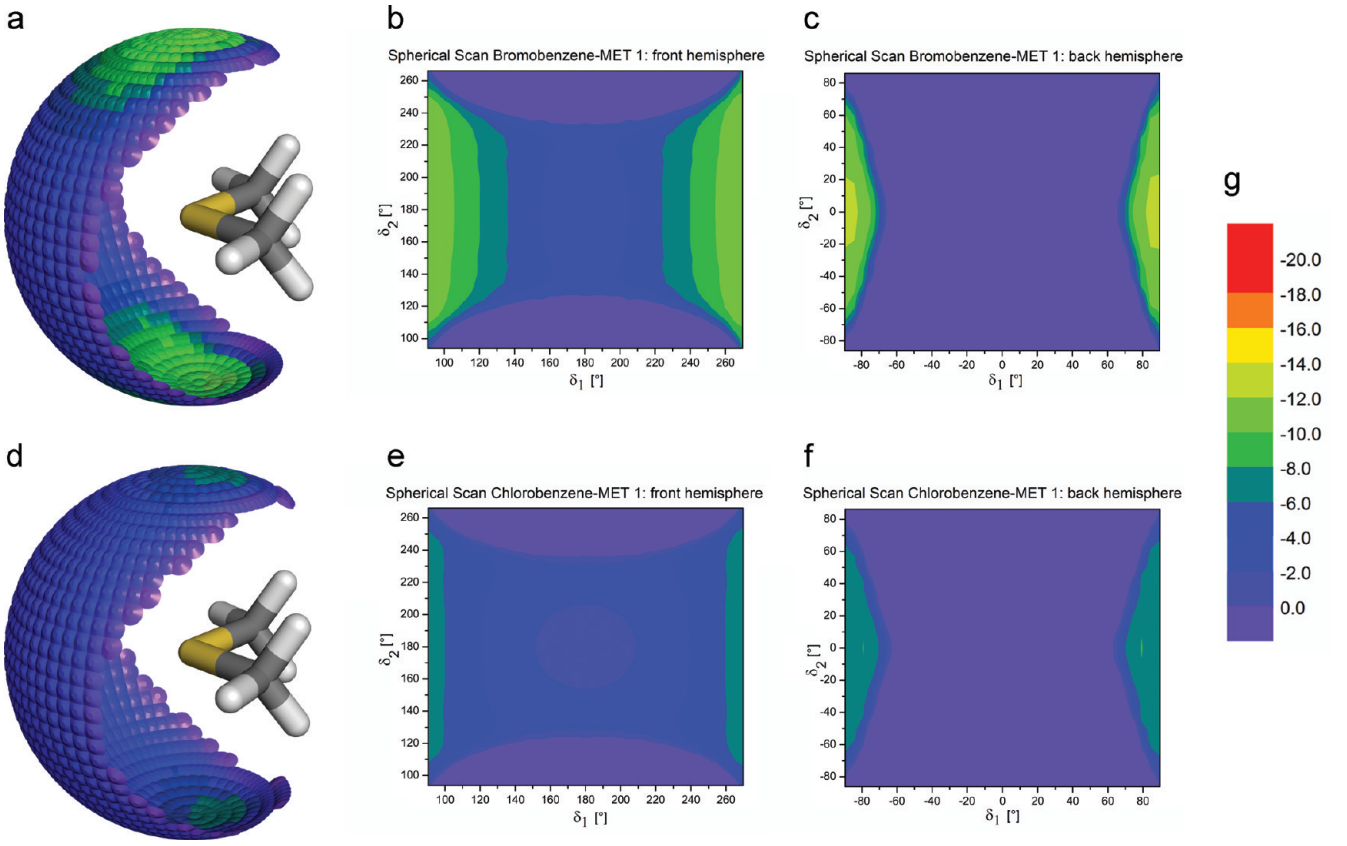

Figure 6. Spherical scans for bromobenzene and chlorobenzene. (a) Interaction energy sphere for the bromobenzene···MET1 complex (b, c) 2D plots (δ1 vs δ2) of interaction energies on the front hemisphere (b) and back hemisphere (c) for the bromobenzene···MET1 complex. (d) Interaction energy sphere for the chlorobenzene···MET1 complex. (e, f) 2D plots (δ1 vs δ2) of interaction energies on the front hemisphere (e) and back hemisphere (f) for the chlorobenzene···MET1 complex. (g) Color scale.

Finally, we also perform spherical scans starting from the unconstrained X···MET1, X···MET2, and X···MET3 geometries. These are shown in the Supporting Information (Figure S5). For the MET1 interaction spheres, we observe a slight loss of symmetry of the energy profiles which can be explained by taking into account that the optimal σ-hole angle $\alpha_{S5-X6-C7}$ is not 180°. This means that two points placed on opposite sides of the sphere are not identical in terms of the σ-hole angle and thus do not lead to the same energies. Increasing the methionine model in size from MET1 to MET2 and MET3, we observe a steady increase of secondary interactions. An obvious example is Figure S5c (Supporting Information), where the areas of favorable interaction are extended toward Cβ and Cγ of the aliphatic side chain. These secondary interactions (mostly CH-π contacts) even outweigh the halogen bond in strength in the Cl···MET3 complex (Supporting Information, Figure S5i). It thus appears that the smallest model system (MET1) is best-suited to describe an isolated halogen bond void of secondary interactions.

DISCUSSION

We have proposed that halogen bonds addressing the sulfur atom of a methionine side chain are favorable interactions that have so far been neglected in molecular and drug design. We have shown that all halobenzene model systems form complexes featuring very similar equilibrium distances. This leads to the assumption that chloro, bromo, and iodo moieties are easily interchangeable as halogen bond partners of the sulfur atom. Our calculations show that the I···S bond is rather strong [CCSD(T) energies of −17.9 kJ/mol or −4.3 kcal/mol], strongest among the halogens, and is superior to weak and moderately strong hydrogen bonds (H···S contacts) when taking ligand desolvation into account. We have elucidated the spatial behavior of halogen bonds by performing scans varying distances, angles, and dihedral angles, deducing simple rules of thumb useful for computational biologists and medicinal chemists alike. In Figure 7 we apply our results by projecting the interaction sphere onto Met39 in the crystal structure of IL-2 with the bound ligand SP4160.[22] The actual geometry of the halogen on the sphere closely matches the optimal interaction area predicted by the calculations (Figure 7a). A comparison with the iodobenzene···MET1 interaction sphere exemplifies how a putative gain of binding energy could be achieved by exchanging chlorine by iodine (Figure 7b,c). It is possible to map these interaction spheres on methionine residues in any crystal structure, enabling medicinal chemists to determine favorable areas of interaction within a binding site and exploit them for scaffold decoration or de novo design.

This work demonstrating the strength of sulfur−halogen bonds has implications not only for gaining compound affinity, but particularly for tuning selectivity. So far, there is no way to address the sulfur atom in a methionine residue selectively and with a directed interaction, as can be achieved through halogen bonding. This allows for novel scaffolds and unorthodox

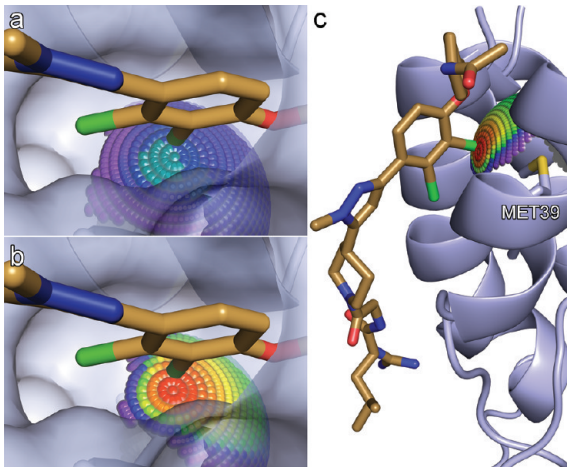

Figure 7. (a) Interaction sphere of chlorobenzene···MET1 mapped onto Met39 in PDB structure 1QVN, illustrating agreement of calculations with an experimentally determined crystal structure. (b) Mapping of the iodobenzene···MET1 interaction sphere onto Met39 exemplifies putative gain of binding energy by exchanging chlorine by iodine. (c) Embedding of halogen-bonding interaction spheres in protein–ligand environments facilitates recognition of preferential binding geometries in molecular design.

approaches in medicinal chemistry. It facilitates exploiting new, patentable chemistry and avoiding already patented chemical space. Finally, our results provide blueprints for integrating sulfur-halogen bonds into molecular design tools.

METHODS

DFT-D and MP2 Structure Optimizations. All DFT and MP2 calculations in this work were performed using the Turbomole 6.2 suite of programs.[25,26] The basis sets used were of triple-ζ (def2-TZVPP)[27] and quadruple-ζ (def2-QZVPP)[27] quality. Relativistic effects for iodine were considered by an effective core potential (ECP).[28] MP2 calculations were done in combination with the resolution of identity (RI) technique[29−32] and the frozen core approximation. The frozen core orbitals were attributed by the default setting in Turbomole, by which all orbitals possessing energies below 3.0 au are considered core orbitals. The SCF convergence criterion was increased to 10^{-8} Hartree for all calculations. Interaction energies were counterpoise-corrected using the procedure of Boys and Bernardi[33] where indicated (Tables 1 and 2) in order to correct for basis set superposition errors (BSSEs). DFT calculations were performed using the RI approximation[34−36] with the BP86,[37,38] BLYP,[37,39] and TPSS[40] functionals. The RI approximation is not efficient for hybrid functionals and hence was not used in B3LYP[37,39,41] calculations. All functionals were augmented with an empirical dispersion correction as proposed by Grimme,[42] which we have indicated by appending "-D" to their names (i.e., BP86-D, BLYP-D, B3LYP-D, TPSS-D). We used the def2-TZVPP[27] basis set throughout, employing a relativistic ECP for iodine.[28]

CCSD(T) Calculations. Structure optimizations for iodobenzene, MET1, and the adduct system were performed with the Turbomole suite employing the SCS-MP2[43] method and the def2-QZVPP[27] basis set. Additionally, we performed MP2 single point calculations with the cc-pVTZ and cc-pVQZ[44−46] basis sets. These MP2 calculations were done in combination with the RI technique[29−32,47] and the frozen core approximation as described above. Relativistic effects for iodine were considered by an effective core potential (ECP).[46]

CCSD(T) calculations were carried out with the cc-pVTZ[44−46] basis set employing the MOLPRO[48] program package. Relativistic effects for iodine were again considered by a relativistic pseudopotential. All CCSD(T) and MP2 energies were counterpoise-corrected using the procedure of Boys and Bernardi.[33] The contribution of higher order correlation energy was determined by the following scheme:[49,50]

$$\Delta E_{\mathrm{CBS}}^{\mathrm{CCSD(T)}} = \Delta E_{\mathrm{CBS}}^{\mathrm{MP2}} + (\Delta E_{\mathrm{cc\text{-}pVTZ}}^{\mathrm{CCSD(T)}} - \Delta E_{\mathrm{cc\text{-}pVTZ}}^{\mathrm{MP2}}) \quad (1)$$

This is based on the assumption that the difference between the CCSD(T) and MP2 interaction energies ($\Delta E^{\mathrm{CCSD(T)}} - \Delta E^{\mathrm{MP2}}$) depends only slightly on basis set size and therefore can be determined with small- or medium-sized basis sets like cc-pVTZ. $\Delta E_{\mathrm{CBS}}^{\mathrm{MP2}}$ is the MP2 energy at the complete basis set limit which was obtained by the extrapolation procedure proposed by Halkier et al.:[51]

$$\Delta E_{\mathrm{CBS}}^{\mathrm{MP2}} = \frac{\Delta E_X^{\mathrm{MP2}} X^3 - \Delta E_Y^{\mathrm{MP2}} Y^3}{X^3 - Y^3} \quad (2)$$

where X and Y are the cardinal numbers of the cc-pVTZ and cc-pVQZ basis set, respectively.

Distance Scans. All distance scans were performed using the optimized MP2/TZVPP geometries as starting points. The bond distances $d_{\mathrm{X}\cdots\mathrm{S}}$ ($d_{\mathrm{H}\cdots\mathrm{S}}$ for benzene) were then elongated or shortened in 2 pm steps (5 pm further away from the minimum), with the rest of the ligand structure (halobenzene or benzene) transformed accordingly. For each step, single-point (SCF) calculations were performed using MP2/TZVPP.

Spherical Scans. Input files were generated from the optimized MP2/TZVPP geometry in C_s symmetry with the angle $\alpha_{\mathrm{S5-X6-C7}}$ restricted to 180° and the dihedral angle $\delta_{\mathrm{C3-C4-S5-X6}}$ restricted to 90° (comparison of minimum geometry and constrained geometry given in Supporting Information, Figure S4). In order to generate a full sphere of input geometries for subsequent calculations, the optimized structure was transformed as follows: The sulfur atom was placed on the origin of the coordinate system and the entire complex was rotated until the halogen atom was positioned on the positive x-axis. Let α denote the angle of rotation counterclockwise around the z-axis and β denote the angle of rotation counterclockwise around the x-axis. α was gradually increased from 0° to 180° in steps of 5°. For each α-value, β was varied from 0° to 355° in steps of 5°, leading to a total number of 2664 halogen positions distributed on a sphere. The structure of the ligand was not altered during this transformation process. Calculations were done as single point (SCF) calculations using the TPSS-D(RI)/TZVPP method.

For visualization purposes, several Python scripts were written and executed in PyMOL.[52] Interaction energies were partitioned into bins and spectrum colors (red to blue to purple) were assigned. At the positions of the halogens small CONE objects with the appropriate coloring were generated. For the 2D plots, 36×36 ($\delta_1 \times \delta_2$) matrices were generated from a worksheet of δ_1, δ_2, and complex formation energy values using the XYZ gridding tool in Origin 8.5 (OriginLab, Northampton, MA). We used "weighted average" as the gridding method with a search radius of 15. Final figures were generated as 2D contour plots.

■ ASSOCIATED CONTENT

Supporting Information. A comparison of MP2 and DFT methods for the complex formation energies and interaction geometries is given in Table S1. The results of the basis set extrapolation procedure to obtain CCSD(T)/CBS energies are given in Table S2. A comparison of the freely optimized geometries for iodobenzene with all three methionine model systems is given in Figure S1. Distance scans with methionine model systems of different sizes are given in Figure S2. A comparison of common DFT-D functionals with MP2 exemplified in the halobenzene−MET1 distance scans is presented in Figure S3. A comparison of the constrained input structures for the spherical scans and freely optimized structures is given in Figure S4, and depictions of interaction spheres from nonconstrained spherical scans are given in Figure S5. This material is available free of charge via the Internet at http://pubs.acs.org.

■ AUTHOR INFORMATION

Corresponding Author

*Phone: +4970712974567. Fax:+497071295637. E-mail: frank.boeckler@uni-tuebingen.de.

■ ACKNOWLEDGMENT

We acknowledge the help of bachelor students Leo Rosenkranz and Alwin Balhuber in the initial stages of this project. High-performance computing resources of the LRZ (Leibniz Rechenzentrum) Munich and of the BW-Grid were kindly made available by the federal states of Bayern and Baden-Wuerttemberg.

■ ABBREVIATIONS:

PDB, Brookhaven Protein Data Bank; QM/MM, quantum mechanics/molecular mechanics; DFT, density functional theory; DFT-D, density functional theory augmented by an empirical dispersion correction; MP2, second-order Møller−Plesset perturbation theory; SCS-MP2, spin-component scaled second-order Møller−Plesset perturbation theory; CCSD(T), coupled-cluster method with single, double and perturbative triple excitations; IL-2, interleukin-2; MET1−MET3, the various models for methionine; Met, methionine; SCF, self-consistent field calculation; ECP, effective core potential; BSSE, basis set superposition error

■ REFERENCES

(1) Bissantz, C.; Kuhn, B.; Stahl, M. A Medicinal Chemist's Guide to Molecular Interactions. *J. Med. Chem.* **2010**, *53*, 5061–5084.

(2) Hassel, O. Structural Aspects of Interatomic Charge-Transfer Bonding. *Science* **1970**, *170*, 497–502.

(3) Pierangelo, M.; Franck, M.; Tullio, P.; Giuseppe, R.; Giancarlo, T. Halogen Bonding in Supramolecular Chemistry. *Angew. Chem., Int. Ed.* **2008**, *47*, 6114–6127.

(4) Auffinger, P.; Hays, F. A.; Westhof, E.; Ho, P. S. Halogen bonds in biological molecules. *Proc. Natl. Acad. Sci. U. S. A.* **2004**, *101*, 16789–16794.

(5) Clark, T.; Hennemann, M.; Murray, J.; Politzer, P. Halogen Bonding: The σ-Hole. *J. Mol. Model.* **2007**, *13*, 291–296.

(6) Murray, J.; Lane, P.; Politzer, P. Expansion of the σ-Hole Concept. *J. Mol. Model.* **2009**, *15*, 723–729.

(7) Murray, J. S.; Lane, P.; Politzer, P. A Predicted New Type of Directional Noncovalent Interaction. *Int. J. Quantum Chem.* **2007**, *107*, 2286–2292.

(8) Murray, J. S.; Riley, K. E.; Politzer, P.; Clark, T. Directional Weak Intermolecular Interactions: σ-Hole Bonding. *Aust. J. Chem.* **2010**, *63*, 1598–1607.

(9) Politzer, P.; Lane, P.; Concha, M.; Ma, Y.; Murray, J. An Overview of Halogen Bonding. *J. Mol. Model.* **2007**, *13*, 305–311.

(10) Murray, J.; Lane, P.; Clark, T.; Politzer, P. σ-Hole Bonding: Molecules Containing Group VI Atoms. *J. Mol. Model.* **2007**, *13*, 1033–1038.

(11) Murray, J. S.; Lane, P.; Politzer, P. Simultaneous Sigma-Hole and Hydrogen Bonding by Sulfur- and Selenium-Containing Heterocycles. *Int. J. Quantum Chem.* **2008**, *108*, 2770–2781.

(12) Riley, K. E.; Hobza, P. Investigations into the Nature of Halogen Bonding Including Symmetry Adapted Perturbation Theory Analyses. *J. Chem. Theory Comput.* **2008**, *4*, 232–242.

(13) Riley, K. E.; Murray, J. S.; Politzer, P.; Concha, M. C.; Hobza, P. Br---O Complexes as Probes of Factors Affecting Halogen Bonding: Interactions of Bromobenzenes and Bromopyrimidines with Acetone. *J. Chem. Theory Comput.* **2009**, *5*, 155–163.

(14) Lu, Y.; Shi, T.; Wang, Y.; Yang, H.; Yan, X.; Luo, X.; Jiang, H.; Zhu, W. Halogen Bonding, a Novel Interaction for Rational Drug Design?. *J. Med. Chem.* **2009**, *52*, 2854–2862.

(15) Lu, Y.; Wang, Y.; Zhu, W. Nonbonding Interactions of Organic Halogens in Biological Systems: Implications for Drug Discovery and Biomolecular Design. *Phys. Chem. Chem. Phys.* **2010**, *12*, 4543–4551.

(16) Voth, A. R.; Khuu, P.; Oishi, K.; Ho, P. S. Halogen Bonds As Orthogonal Molecular Interactions to Hydrogen Bonds. *Nat. Chem.* **2009**, *1*, 74–79.

(17) Politzer, P.; Murray, J. S.; Lane, P. Sigma-Hole Bonding and Hydrogen Bonding: Competitive Interactions. *Int. J. Quantum Chem.* **2007**, *107*, 3046–3052.

(18) Shields, Z. P.; Murray, J. S.; Politzer, P. Directional Tendencies of Halogen and Hydrogen Bonds. *Int. J. Quantum Chem.* **2010**, *110*, 2823–2832.

(19) Politzer, P.; Murray, J. S.; Clark, T. Halogen Bonding: An Electrostatically-Driven Highly Directional Noncovalent Interaction. *Phys. Chem. Chem. Phys.* **2010**, *12*, 7748–7757.

(20) Fedorov, O.; Huber, K.; Eisenreich, A.; Filippakopoulos, P.; King, O.; Bullock, A. N.; Szklarczyk, D.; Jensen, L. J.; Fabbro, D.; Trappe, J.; Rauch, U.; Bracher, F.; Knapp, S. Specific CLK Inhibitors from a Novel Chemotype for Regulation of Alternative Splicing. *Chem. Biol.* **2011**, *18*, 67–76.

(21) Hardegger, L. A.; Kuhn, B.; Spinnler, B.; Anselm, L.; Ecabert, R.; Stihle, M.; Gsell, B.; Thoma, R.; Diez, J.; Benz, J.; Plancher, J.-M.; Hartmann, G.; Banner, D. W.; Haap, W.; Diederich, F. Systematic Investigation of Halogen Bonding in Protein−Ligand Interactions. *Angew. Chem., Int. Ed.* **2011**, *50*, 314–318.

(22) Thanos, C. D.; DeLano, W. L.; Wells, J. A. Hot-Spot Mimicry of a Cytokine Receptor by a Small Molecule. *Proc. Natl. Acad. Sci. U. S. A.* **2006**, *103*, 15422–15427.

(23) Liu, L.; Baase, W. A.; Matthews, B. W. Halogenated Benzenes Bound within a Non-Polar Cavity in T4 Lysozyme Provide Examples of I···S and I···Se Halogen-Bonding. *J. Mol. Biol.* **2009**, *385*, 595–605.

(24) Estébanez-Perpiñá, E.; Arnold, L. A.; Nguyen, P.; Rodrigues, E. D.; Mar, E.; Bateman, R.; Pallai, P.; Shokat, K. M.; Baxter, J. D.; Guy, R. K.; Webb, P.; Fletterick, R. J. A surface on the androgen receptor that allosterically regulates coactivator binding. *Proc. Natl. Acad. Sci. U. S. A.* **2007**, *104*, 16074–16079.

(25) Ahlrichs, R.; Bär, M.; Häser, M.; Horn, H.; Kölmel, C. Electronic Structure Calculations on Workstation Computers: The Program System Turbomole. *Chem. Phys. Lett.* **1989**, *162*, 165–169.

(26) Turbomole v6.2 (June 2010), available from http://www.turbomole.com. 2010.

(27) Weigend, F.; Ahlrichs, R. Balanced Basis Sets of Split Valence, Triple Zeta Valence and Quadruple Zeta Valence Quality for H to Rn: Design and Assessment of Accuracy. *Phys. Chem. Chem. Phys.* **2005**, *7*, 3297–3305.

(28) Peterson, K. A.; Figgen, D.; Goll, E.; Stoll, H.; Dolg, M. Systematically Convergent Basis Sets with Relativistic Pseudopotentials. II. Small-Core Pseudopotentials and Correlation Consistent Basis Sets

for the Post-d Group 16−18 Elements. *J. Chem. Phys.* **2003**, *119*, 11113–11123.

(29) Feyereisen, M.; Fitzgerald, G.; Komornicki, A. Use of Approximate Integrals in Ab Initio Theory. An Application in MP2 Energy Calculations. *Chem. Phys. Lett.* **1993**, *208*, 359–363.

(30) Weigend, F.; Häser, M.; Patzelt, H.; Ahlrichs, R. RI-MP2: Optimized Auxiliary Basis Sets and Demonstration of Efficiency. *Chem. Phys. Lett.* **1998**, *294*, 143–152.

(31) Hättig, C. Optimization of Auxiliary Basis Sets for RI-MP2 and RI-CC2 Calculations: Core-Valence and Quintuple-ζ Basis Sets for H to Ar and QZVPP Basis Sets for Li to Kr. *Phys. Chem. Chem. Phys.* **2005**, *7*, 59–66.

(32) Hellweg, A.; Hättig, C.; Höfener, S.; Klopper, W. Optimized Accurate Auxiliary Basis Sets for RI-MP2 and RI-CC2 Calculations for the Atoms Rb to Rn. *Theor. Chem. Acc.* **2007**, *117*, 587–597.

(33) Boys, S. F.; Bernardi, F. The calculation of small molecular interactions by the differences of separate total energies. Some procedures with reduced errors. *Mol. Phys.* **1970**, *19*, 553–566.

(34) Baerends, E. J.; Ellis, D. E.; Ros, P. Self-Consistent Molecular Hartree−Fock−Slater Calculations I. The Computational Procedure. *Chem. Phys.* **1973**, *2*, 41–51.

(35) Dunlap, B. I.; Connolly, J. W. D.; Sabin, J. R. On Some Approximations in Applications of X Alpha Theory. *J. Chem. Phys.* **1979**, *71*, 3396–3402.

(36) Weigend, F. Accurate Coulomb-Fitting Basis Sets for H to Rn. *Phys. Chem. Chem. Phys.* **2006**, *8*, 1057–1065.

(37) Becke, A. D. Density-Functional Exchange-Energy Approximation with Correct Asymptotic Behavior. *Phys. Rev. A* **1988**, *38*, 3098.

(38) Perdew, J. P. Density-Functional Approximation for the Correlation Energy of the Inhomogeneous Electron Gas. *Phys. Rev. B* **1986**, *33*, 8822.

(39) Lee, C.; Yang, W.; Parr, R. G. Development of the Colle−Salvetti Correlation-Energy Formula into a Functional of the Electron Density. *Phys. Rev. B* **1988**, *37*, 785.

(40) Staroverov, V. N.; Scuseria, G. E.; Tao, J.; Perdew, J. P. Comparative Assessment of a New Nonempirical Density Functional: Molecules and Hydrogen-Bonded Complexes. *J. Chem. Phys.* **2003**, *119*, 12129–12137.

(41) Becke, A. D. Density-Functional Thermochemistry. III. The Role of Exact Exchange. *J. Chem. Phys.* **1993**, *98*, 5648–5652.

(42) Grimme, S. Semiempirical GGA-type Density Functional Constructed with a Long-Range Dispersion Correction. *J. Comput. Chem.* **2006**, *27*, 1787–1799.

(43) Grimme, S. Improved Second-Order Møller−Plesset Perturbation Theory by Separate Scaling of Parallel- and Antiparallel-Spin Pair Correlation Energies. *J. Chem. Phys.* **2003**, *118*, 9095–9102.

(44) Dunning, J. T. H. Gaussian basis sets for use in correlated molecular calculations. I. The atoms boron through neon and hydrogen. *J. Chem. Phys.* **1989**, *90*, 1007–1023.

(45) Woon, D. E.; Dunning, J. T. H. Gaussian Basis Sets for Use in Correlated Molecular Calculations. III. The Atoms Aluminum through Argon. *J. Chem. Phys.* **1993**, *98*, 1358–1371.

(46) Peterson, K. A.; Shepler, B. C.; Figgen, D.; Stoll, H. On the Spectroscopic and Thermochemical Properties of ClO, BrO, IO, and Their Anions. *J. Phys. Chem. A* **2006**, *110*, 13877–13883.

(47) Weigend, F.; Kohn, A.; Hättig, C. Efficient Use of the Correlation Consistent Basis Sets in Resolution of the Identity MP2 Calculations. *J. Chem. Phys.* **2002**, *116*, 3175–3183.

(48) Werner, H.-J.; Knowles, P. J.; Lindh, R.; Manby, F. R.; Schütz, M.; Celani, P.; Korona, T.; Rauhut, G.; Amos, R. D.; Bernhardsson, A.; Berning, A.; Cooper, D. L.; Deegan, M. J. O.; Dobbyn, A. J.; Eckert, F.; Hampel, C.; Hetzer, G.; Lloyd, A. W.; McNicholas, S. J.; Meyer, W.; Mura, M. E.; Nicklass, A.; Palmieri, P.; Pitzer, R.; Schumann, U.; Stoll, H.; Stone, A. J.; Tarroni, R.; Thorsteinsson, T. MOLPRO, version 2006.1, a package of ab initio programs; http://www.molpro.net. 2006.

(49) Hobza, P.; Šponer, J. Toward True DNA Base-Stacking Energies: MP2, CCSD(T), and Complete Basis Set Calculations. *J. Am. Chem. Soc.* **2002**, *124*, 11802–11808.

(50) Jurecka, P.; Sponer, J.; Cerny, J.; Hobza, P. Benchmark Database of Accurate (MP2 and CCSD(T) complete basis set limit) Interaction Energies of Small Model Complexes, DNA Base Pairs, And Amino Acid Pairs. *Phys. Chem. Chem. Phys.* **2006**, *8*, 1985–1993.

(51) Halkier, A.; Helgaker, T.; Jørgensen, P.; Klopper, W.; Koch, H.; Olsen, J.; Wilson, A. K. Basis-Set Convergence in Correlated Calculations on Ne, N_2, and H_2O. *Chem. Phys. Lett.* **1998**, *286*, 243–252.

(52) DeLano, W. L. *The PyMOL Molecular Graphics System*; DeLano Scientific LLC: Palo Alto, CA, USA. 2008.